Earth and Planetary Science Letters 299 (2010) 483–495

Contents lists available at ScienceDirect

Earth and Planetary Science Letters

journal homepage: www.elsevier.com/locate/epsl

Eocene sea temperatures for the mid-latitude southwest Pacific from Mg/Ca ratios in planktonic and benthic foraminifera

John B. Creech [a,*], Joel A. Baker [a], Christopher J. Hollis [b], Hugh E.G. Morgans [b], Euan G.C. Smith [c]

[a] School of Geography, Environment and Earth Sciences, Victoria University of Wellington, P.O. Box 600, Wellington, New Zealand
[b] GNS Science, P.O. Box 30368, Lower Hutt 5040, New Zealand
[c] Institute of Geophysics, Victoria University of Wellington, P.O. Box 600, Wellington, New Zealand

ARTICLE INFO

Article history:
Received 18 May 2010
Received in revised form 23 September 2010
Accepted 23 September 2010
Available online 18 October 2010

Editor: P. DeMenocal

Keywords:
Early Eocene
Mg/Ca
paleoclimate
EECO
foraminifera
LA-ICP-MS

ABSTRACT

We have used laser ablation inductively coupled plasma mass spectrometry (LA-ICP-MS) to measure elemental (Mg/Ca, Al/Ca, Mn/Ca, Zn/Ca, Sr/Ca, and Ba/Ca) ratios of 13 species of variably preserved early to middle Eocene planktonic and benthic foraminifera from New Zealand. The foraminifera were obtained from Ashley Mudstone, mid-Waipara River, South Island, which was deposited at bathyal depth (*ca.* 1000 m) on the northern margin of the east-facing Canterbury Basin at a paleo-latitude of *ca.* 55°S. LA-ICP-MS data yield trace element depth profiles through foraminifera test walls that can be used to identify and exclude zones of surficial contamination and infilling material resulting from diagenetic coatings, mineralisation and detrital sediment. Screened Mg/Ca ratios from 5 species of foraminifera are used to calculate sea temperatures from late Early to early Middle Eocene (*ca.* 51 to 46.5 Ma), a time interval that spans the termination of the Early Eocene Climatic Optimum (EECO). During this time, sea surface temperatures (SST) varied from 30 to 24 °C, and bottom water temperatures (BWT) from 21 to 14 °C. Comparison of Mg/Ca sea temperatures with published $\delta^{18}O$ and TEX_{86} temperature data from the same samples (Hollis et al., 2009) shows close correspondence, indicating that LA-ICP-MS can provide reliable Mg/Ca sea temperatures even where foraminiferal test preservation is variable. Agreement between the three proxies also implies that Mg/Ca-temperature calibrations for modern planktonic and benthic foraminifera can generally be applied to Eocene species, although some species (e.g., *V. marshalli*) show significant calibration differences. The Mg/Ca ratio of the Eocene ocean is constrained by our data to be 35–50% lower than the modern ocean depending on which TEX_{86} – temperature calibration (Kim et al., 2008; Liu et al., 2009) – is used to compare with the Mg/Ca sea temperatures. Sea temperatures derived from $\delta^{18}O$ analysis of foraminifera from Waipara show amplified variability relative to the Mg/Ca and TEX_{86} proxies. This amplified variability is probably a diagenetic effect although it is possible that this Eocene $\delta^{18}O$ record contains an ice volume component — the amplification signalling that temperature changes may have been accompanied by growth and collapse of ephemeral polar ice sheets on timescales of *ca.* 0.5 Myr.

1. Introduction

Sea temperature estimates derived from magnesium/calcium (Mg/Ca) ratios, based on the thermodynamically controlled incorporation of Mg into the calcite tests of foraminifera, are widely used as a tool for reconstructing past climates (Billups and Schrag, 2003; Burgess et al., 2008; Lear et al., 2000, 2008; Mashiotta et al., 1999; Tripati and Elderfield, 2005; Tripati et al., 2003). Most previous applications of the Mg/Ca thermometer have utilized bulk analytical methods where several foraminifer tests are crushed, chemically cleaned with oxidizing (±reducing) agents, dissolved in acid and then analysed in solution. These methods require careful cleaning procedures to remove potential contaminant phases and detritus that may affect the measured test chemistry and could potentially result in erroneous paleo-sea temperatures. These methods also provide only a single temperature for each sample.

Advances in micro-analytical techniques, including laser ablation inductively coupled plasma mass spectrometry (LA-ICP-MS), now enable precise *in situ* analysis of trace elements in foraminifer tests at a spatial resolution of a few tens of microns. As the laser spot size is small relative to the size of foraminifer tests, this type of analysis permits multiple analyses to be made on a single specimen or even within a single test chamber. This can reveal both inter- and intra-individual trace element heterogeneity related to factors such as ecological or vital effects (Eggins et al., 2003, 2004; Reichart et al., 2003; Sadekov et al., 2008, 2009). One particularly useful feature of laser ablation analysis is that it yields a trace element depth profile through the foraminifer test wall that can be used to identify and

* Corresponding author.
E-mail address: john.creech@vuw.ac.nz (J.B. Creech).

0012-821X/$ – see front matter © 2010 Elsevier B.V. All rights reserved.
doi:10.1016/j.epsl.2010.09.039

exclude zones of surficial and internal contamination resulting from diagenetic coatings, mineralisation and presence of detrital sediment (Eggins et al., 2003). Thus, this method is particularly suited to the study of foraminifera from older sediments where the degree of preservation and effects of diagenesis may potentially compromise chemical and isotopic analyses of foraminifera by bulk analytical methods (e.g. Pearson et al., 2001).

In this study, we demonstrate how trace element data obtained by LA-ICP-MS can be utilized to estimate sea temperatures from Eocene foraminifera. These foraminifera were obtained from a river bank section through Ashley Mudstone at Mid-Waipara River, north Canterbury, South Island (Morgans et al., 2005). Ashley Mudstone is a calcareous mudstone that is inferred to have been deposited in upper bathyal depths at a paleo-latitude of *ca*. 55°S. Biostratigraphic data indicate that the sampled interval represents continuous deposition from *ca*. 51 to 46.5 Ma (Hollis et al., 2009). This time interval spans the termination of an interval of extreme global warmth that is referred to as the Early Eocene Climatic Optimum (EECO) and extends from *ca*. 53 to 50 Ma (Zachos et al., 2001). The EECO was followed by a 17 Myr cooling trend, representing the transition from greenhouse to icehouse conditions. Oxygen isotope records indicate that ocean temperatures were much higher than today during the EECO (e.g. Shackleton and Boersma, 1981; Zachos et al., 2001). Coupled benthic Mg/Ca–$\delta^{18}O$ studies suggest that variations in $\delta^{18}O$ during the Early Eocene primarily reflect changes in temperature and that there was no significant continental ice (Billups and Schrag, 2003; Lear et al., 2000).

Hollis et al. (2009) presented geochemical and paleontological evidence for tropical sea surface temperatures in the Eocene at southern mid-latitudes from the same suite of 20 samples that are used in this study. However, those sea temperature estimates were primarily based on TEX_{86} (18 samples) and oxygen isotopes (13 samples), with Mg/Ca data presented for only 5 samples of 3 species of foraminifera. Here we present a greatly expanded set of trace element data for up to 13 species of foraminifera taken from 19 of the Eocene samples. We compare our Mg/Ca sea temperature estimates with the TEX_{86} and oxygen isotope data of Hollis et al. (2009). This comparison makes it possible to assess: (1) the potential of LA-ICP-MS to recover reliable trace element chemistry and sea temperatures from early Cenozoic foraminifera; (2) the validity of using Mg/Ca-temperature calibrations from modern foraminifera for extinct Eocene species; (3) the Mg/Ca ratio of Eocene seawater. Our results also provide new insights into the transition from the Eocene greenhouse world to cooler climates and tentatively suggest that substantive ephemeral continental ice sheets may have developed periodically just after the EECO.

2. Samples and existing comparative data

A Cretaceous–Cenozoic sedimentary succession outcrops along the banks and within the bed of the middle branch of the Waipara River (mid-Waipara) in north Canterbury. A 60 m section of Eocene Ashley Mudstone is exposed in the river bed a few hundred metres upstream from the lower gorge (New Zealand topographic 1:50,000 map series grid reference M34/783949 to 784947) (Column 6 in Morgans et al., 2005; see Table S1 in Supplementary information). The Ashley Mudstone ranges in age from Early to Middle Eocene (Waipawan to Bortonian local stages). It is inferred to conformably overlie the Paleocene Waipara Greensand and is unconformably overlain by the Karetu Sandstone (King et al., 1999). Early collections from this section (Jenkins, 1971) suggest that an intact Paleocene–Eocene boundary interval may lie directly downstream of the Ashley Mudstone exposure but it is currently buried under river scree. Neither the base nor top of the Ashley Mudstone is currently exposed in the section. A suite of 51 samples was collected in 2003 (Morgans et al., 2005) and subsets of these samples have been used to establish the age range of the section utilising calcareous nannofossil, foraminiferal, radiolarian and dinoflagellate cyst biostratigraphy (Hollis et al., 2009). The age model is based on age assignments for bioevents and New Zealand local stage boundaries given in Cooper (2004), which for the Paleogene is calibrated to Berggren et al. (1995). The Ashley Mudstone is inferred to have been deposited in a neritic watermass at upper bathyal depths of *ca*. 1000 m (Hollis et al., 2009). Palinspastic reconstructions of New Zealand during the Early Eocene place the New Zealand landmass between *ca*. 50° and 60° south (Hollis et al., 2009), approximately 10° further south than the present day (Fig. 1).

Foraminifera from a suite of 20 samples from the mid-Waipara section were prepared for geochemical analysis. In addition to the trace element data presented in this study, splits from the same samples have previously been analysed for oxygen and carbon isotopes (foraminifera) and TEX_{86} (archaeal membrane lipids) (Hollis et al., 2009). The degree of preservation of the foraminifera decreases markedly upward through the section, as documented by scanning electron microscope images (Fig. 2). A total of 13 species of foraminifera have been analysed in this study, comprising 5 planktonic species (*Morozovella crater, M. lensiformis, Acarinina primitiva, A. collactea* and *Pseudohastigerina wilcoxensis*) and 9 benthic species (*Elphidium hampdenense, Anomalina visenda, Nuttallides carinotruempyi, Cibicides pre-parki, C.* sp. A, *C. collinsi, Vaginulinopsis marshalli, Bulimina subbortonica*).

Knowledge of the ecology of Eocene foraminifera is limited. Morozovellids are generally considered to be warm-water indicators and are common in (sub)tropical areas. A near-surface mixed-layer habitat is indicated by oxygen and carbon isotopes (Berggren and Pearson, 2006; Boersma et al., 1987; Quilléveré et al., 2001). *A. collactea* is a cosmopolitan species, ranging into latitudes >50° in both hemispheres, while *A. primitiva* is essentially a temperate, high latitude species with an austral–subantarctic distribution (Berggren et al., 2006), and most acarininids are considered to be mixed-layer dwellers with carbon isotopes suggesting a photosymbiotic life habitat (Berggren et al., 2006; Quilléveré et al., 2001). *P. wilcoxensis* is restricted to mid- to high latitudes. Studies of *Pseudohastigerina* taxa suggest a shallow water habitat (Poore and Matthews, 1984). Hayward et al. (1997) consider the benthic genus *Elphidium* to be mostly free-living, epifaunal, sometimes adopting a clinging lifestyle, and predominantly herbivorous (pinnate diatoms) although it sometimes can be detrivorous. However, given its occurrence in mainly bathyal sediments, *E. hampdenense* appears to have had quite a different habitat to most other species in the genus, which are restricted to shallow coastal waters. *Bulimina* is considered to be an infaunal taxon, and *Vaginulinopsis* (elongate nodosariid) is thought to have a similar habitat. Rotaline genera such as *Cibicides* and *Nuttallides* with flattened sides or with some sculpture may have some attaching epifaunal habitat either above or at the sediment–water interface.

In the previous study of sea temperature variation in this section (Hollis et al., 2009), temperature estimates from $\delta^{18}O$ were based on analyses of single specimens of foraminifera with the planktonic genus *Morozovella* used as an indicator of near-surface sea temperatures (SST) and the benthic genus *Cibicides* used as an indicator for sea-floor bottom water temperatures (BWT), which is thought to represent intermediate water in this upper bathyal setting (Hollis et al., 2009). Temperatures were estimated using the equation of Erez and Luz (1983) assuming an ice-free $\delta^{18}O_{seawater}$ value of −1‰ (Zachos et al., 1994). No corrections were made for surface-water salinity or other isotopic fractionation effects.

TEX_{86} SST estimates (Hollis et al., 2009) were based on the relative distribution of glycerol dialkyl glycerol tetraether (GDGT) in membrane lipids from the marine picoplankton *Crenarchaeota* (Schouten et al., 2002, 2007), using the Kim et al. (2008) global calibration from core-top data that assumes a linear relationship between water temperature and TEX_{86} values. However, Liu et al. (2009) have argued that the exclusion of some core-top locations and outliers from the

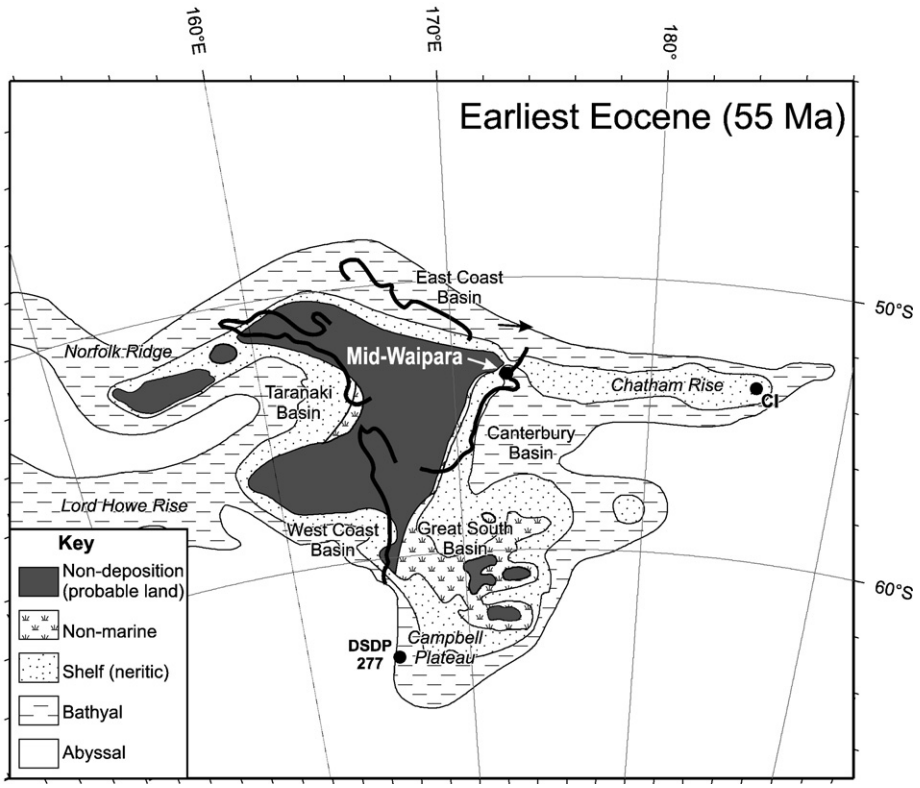

Fig. 1. Paleogeographic map of New Zealand during the Early Eocene at *ca.* 55 Ma (after Hollis et al., 2009). At this time, the New Zealand landmass was situated *ca.* 10° further south than the present day and the mid-Waipara locality would have been at *ca.* 54°S.

linear calibration narrows its geological application, and have produced a non-linear calibration from the same core-top sample set that fits all of the available data. Bijl et al. (2009) have subsequently argued that the exclusion of some data is appropriate due to the different behaviour of *Crenarchaeota* in some special settings and have continued to use the Kim et al. (2008) calibration. In this study, the TEX_{86} data from Hollis et al. (2009) have been converted into SSTs using both of these calibrations, and the differences between them are subsequently discussed.

A new TEX_{86} calibration was recently published by Kim et al. (2010), which addresses the application of these calibrations to high sea surface temperatures. The authors present two calibrations that represent fits to core-top TEX_{86} data from two groups of sites with different temperature ranges. The authors suggest that samples from a greenhouse world ocean, such as those from this study, be calibrated using their high temperature calibration, which was found to produce good agreement with $\delta^{18}O$ data from planktonic foraminifera. Re-calculation of TEX_{86} temperatures using this calibration results in values that are intermediate between those calculated using the Kim et al. (2008) and Liu et al. (2009) calibrations — lower than the latter but higher than the former.

3. Analytical techniques

3.1. Sample preparation

To recover foraminifera, samples of *ca.* 500 g of bulk sediment were dried at <40 °C, and washed over a 75 μm screen, dried again at <40 °C, and the residue weighed and split for census data and faunal slides. Selected taxa were picked from faunal slides and prepared for LA-ICP-MS trace element analysis. Prior to analysis, all foraminifera tests were cleaned to remove adhering clay and other detrital material by repeated rinsing in ultra-pure (>18.2 MΩ) water and analytical reagent (AR) grade methanol. The cleaning procedure did not include an ultrasonication step as these Eocene specimens were found to easily disintegrate, and given the small number of specimens available, the risk of sample loss outweighed the potential benefit of removing small amounts of adhered/infilling material. Individual foraminifera were mounted onto double-sided tape attached to the surface of a wafer of National Institute of Standards and Technology glass standard NIST610 (Jochum and Stoll, 2008; Pearce et al., 1997).

3.2. LA-ICP-MS trace element analysis

Foraminifera were ablated with a New Wave 193 nm laser ablation system using a 25 μm spot size and laser repetition rate of 2 or 3 Hz and laser power of ~50%. Under these conditions, a laser ablation pit is gradually ablated at a rate of ~0.2 to 0.3 μm s^{-1}, yielding a trace element depth profile through the test. Ablation was carried out in a helium atmosphere and the ablated material carried to the ICP-MS torch in a helium–argon gas mixture. An Agilent 7500CS ICP-MS was used to measure trace element abundances relative to Ca during ablation. The isotopes ^{24}Mg, ^{27}Al, ^{43}Ca, ^{55}Mn, ^{66}Zn, ^{88}Sr and ^{138}Ba were repeatedly scanned during ablation with dwell times of 10 ms. Instrumental backgrounds of 60 s were determined prior to each analysis, which was typically 120 s long. Analyses of the NIST610 glass were interspersed between every 5–10 analyses of foraminifera to correct for trace element fractionation induced by the laser ablation and mass spectrometry procedures. Typical foraminifera (foram) and background (bg) rates (cps) were: $^{24}Mg_{foram} = 60\,000$, $^{24}Mg_{bg} = 300$; $^{27}Al_{foram} = 160\,000$, $^{27}Al_{bg} = 5000$; $^{43}Ca_{foram} = 42\,000$, $^{43}Ca_{bg} = 300$; $^{55}Mn_{foram} = 14\,000$, $^{55}Mn_{bg} = 5000$; $^{66}Zn_{foram} = 700$, $^{66}Zn_{bg} = 40$; $^{88}Sr_{foram} = 85\,000$, $^{88}Sr_{bg} = 20$; $^{138}Ba_{foram} = 8000$, and $^{138}Ba_{bg} = 20$.

After LA-ICP-MS analysis, the foraminifera were carbon coated and imaged by scanning electron microscopy (SEM) to compare laser pits

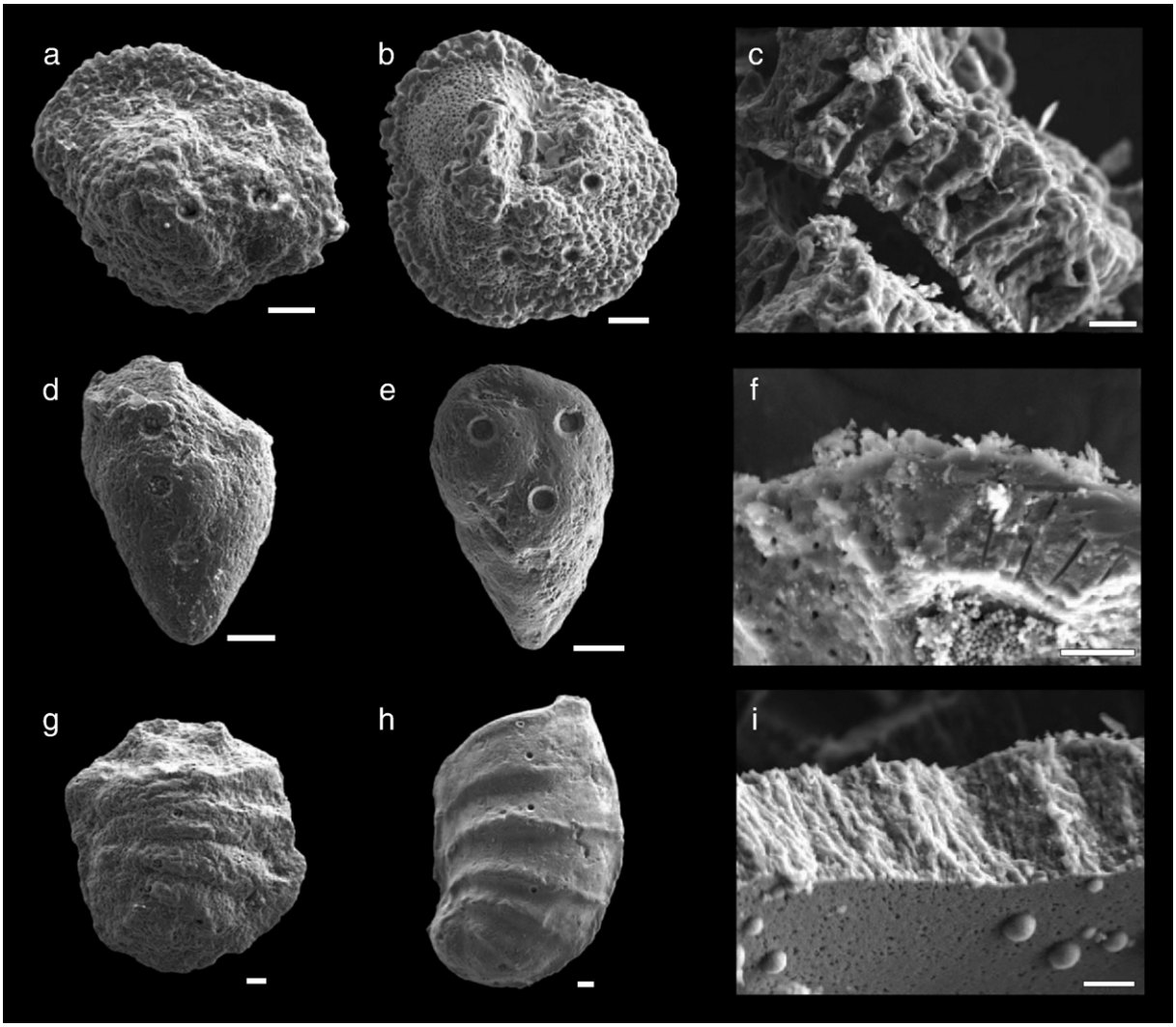

Fig. 2. Scanning electron microscope images illustrating the variable preservation of mid-Waipara planktonic and benthic foraminifer tests. (a–c) = *M. crater*; (d–f) = *B. subbortonica*; (g–i) = *V. marshalli*; (a), (d) and (g) are specimens from the upper part of the section where foraminifera are poorly preserved; (b), (e) and (h) are specimens from the lower part of the section where foraminifera are relatively well preserved; (c), (f) and (i) are images of cross-sections of test walls from relatively well preserved specimens. Diagenetic overgrowths are clearly visible in (c) and (f), showing that even the well preserved specimens have been diagenetically affected. The white scale bars on the whole specimens and wall cross-sections are 50 μm and 20 μm, respectively.

with their respective analyses to assess the preservation of foraminifer specimens and quality of each analysis.

3.3. Data reduction and screening

Element/Ca ratios were plotted versus ablation time, producing a depth profile of foraminifera test chemistry from its exterior through to the interior (Fig. 3). Trace element profiles were then screened for the effects of diagenesis and contamination. Most trace element profiles show an enriched zone of high Mg/Ca at the start of each analysis, followed by an interval of relatively constant and lower Mg/Ca, consistent with observations reported in previous *in situ* laser ablation studies of foraminifera (e.g. Eggins et al., 2003; Pena et al., 2005; Reichart et al., 2003; Sadekov et al., 2008). Ablating further into the interior of the foraminifer generally results in a return to high Mg/Ca values, indicating that the laser has penetrated the inner wall of the test and is ablating infilling clay and/or secondary minerals. Zones of high Mg/Ca are also typically marked by high Al/Ca and Mn/Ca. For the purposes of calculating Mg/Ca sea temperatures, the enriched outer and inner zones are excluded from the mean and just the interval of constant and low Mg/Ca, representing the primary foraminiferal calcite, is averaged (Fig. 3). Depth profiles were found to vary significantly between species due to varying properties (thickness, density etc.) of tests from different taxa. Benthic species generally yield better laser ablation profiles as a result of ablation of their denser, less porous, less ornamented, and flatter tests. Some species (particularly *V. marshalli*) consistently produced long, regular depth profiles, of which the integrated segment comprised most of the analysis (Fig. 3A).

After screening of depth profiles, summary trace element data was scrutinized, and analyses with anomalously high values in any trace element were also discarded. Unscreened data also shows a linear correlation between Mg/Ca and Al/Ca, which reflects the influence of silicate contamination (interpreted as small amounts of sediment infilling pores). Following Barker et al. (2003), the composition of the contaminant can be approximately determined by plotting Mg/Ca versus Al/Ca, from which the slope of a linear regression gives the Al/Mg ratio of the sediment. Once the contaminant composition is known, screening limits for silicate contamination can be set by calculating the Al/Ca ratio at which Mg/Ca would be biased sufficient to alter temperatures by >1 °C. The sediment composition from the mid-Waipara samples was determined from a plot of all unscreened data from all species, excluding only analyses with extreme values of Al/Ca (>50 mmol/mol). This yielded an Al/Mg ratio of 8.1 (i.e. much less Mg-rich than the sediment in Barker et al. (2003)) from which screening limits were calculated for

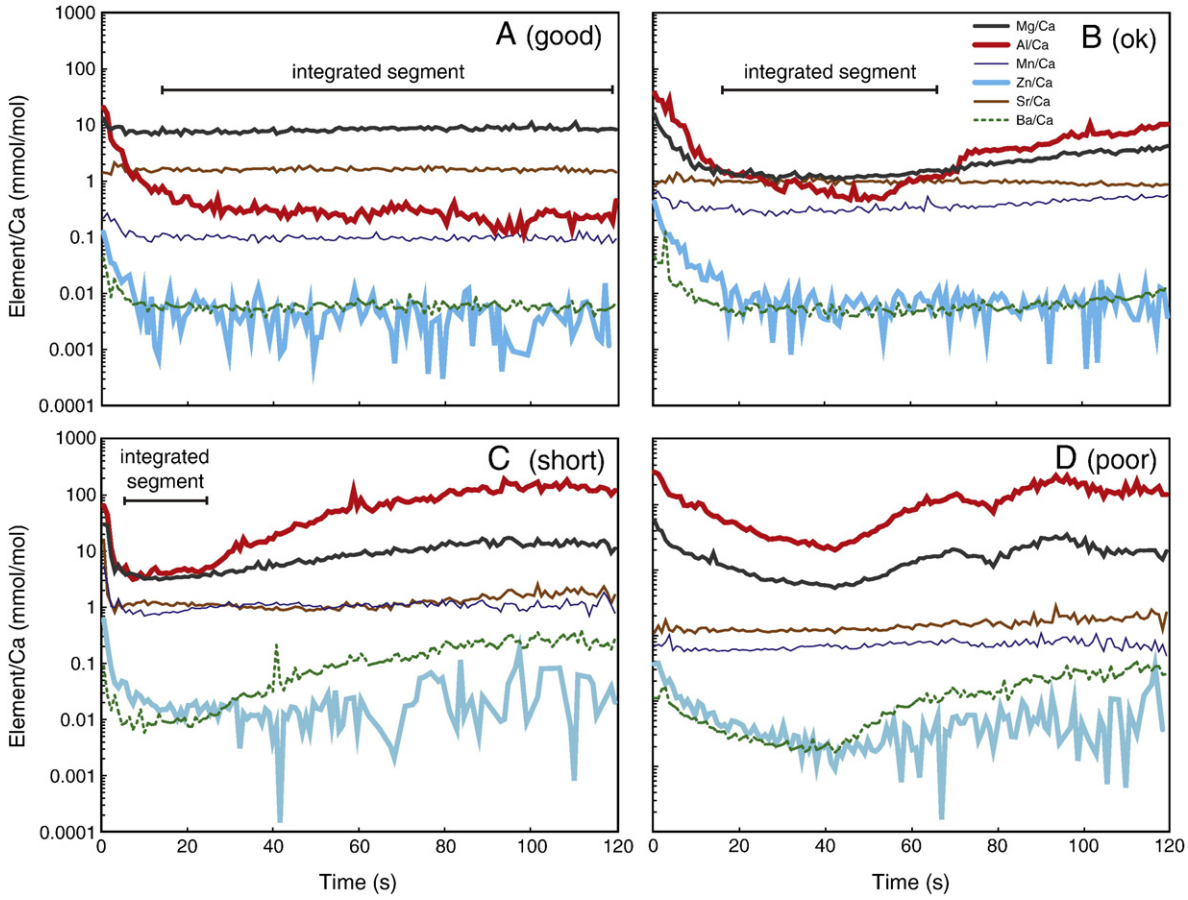

Fig. 3. Examples of LA-ICP-MS trace element depth profiles showing the different types of profiles through foraminifera test walls and how these are screened to yield reliable Mg/Ca data. The lower scale on the profiles is ablation time, which corresponds to a depth of *ca.* 0.2–0.3 μm s^{-1}. In profiles (A–C) a surface veneer that is enriched in trace elements is clearly evident. This is followed by an interval of variable thickness characterized by low and relatively constant Mg/Ca, which is interpreted to be the part of the profile reflecting primary foraminiferal calcite chemistry that is averaged for the calculation of Mg/Ca paleo-sea temperatures. The deeper part of most profiles typically shows a return to higher trace element/Ca values that may indicate that the laser is ablating material infilling chambers or secondary minerals. (A) is an example of a "good" profile where the segment that can be used for temperature determination comprises most of the analysis, which was typical of the benthic species *V. marshalli*, but was less common for other taxa; (B) is a "fair" profile where the usable segment is perhaps half of the analysis, which was common amongst most species analysed in this study; (C) is a "short" profile typical of the more delicate benthic species such as *B. subbortonica* where only a limited part of the profile represents the primary trace element signal of the foraminiferal calcite; (D) is an example of a "bad" profile that would not be used in this study, as was the case for a significant number of analyses of planktonic taxa, particularly towards the top of the mid-Waipara section.

each species. The screening limit also depends on the calibration used (i.e. planktonic or benthic) and the typical Mg/Ca ratio for each species. For example, the planktonic species *M. crater* has a typical Mg/Ca value of ca. 3.6 mmol/mol. Based on the planktonic calibration, an increase of 9% (0.325 mmol/mol) Mg/Ca would increase the calculated temperature by 1 °C. Based on the equation of Barker et al. (2003) $Mg/Ca_{(excess)} = Al/Ca_{(sample)} / Al/Mg_{(contaminant)}$), the required limit for Al/Ca in this case is $0.325 \times 8.1 = 2.6$ mmol/mol. Thus, when the data are screened in this way, no analysis should overestimate temperature by more than 1 °C. For the detailed temperature–time records presented in Section 4.1, each species was screened with individual Al/Ca limits (mmol/mol) of 2.6 for *M. crater*, 2.3 for *A. primitiva*, 3.5 for *Cibicides* sp. A, 2.5 for *B. subbortonica*, and 7.2 for *V. marshalli* (see Supplementary information).

3.4. Calculating Mg/Ca paleo-sea temperatures

The Mg/Ca ratio is related to water temperature by the equation:

$$Mg/Ca = (Mg/Ca_{sw-t} / Mg/Ca_{sw-0}) \times B \times e^{(A \times T)}$$

Mg/Ca_{sw} is seawater Mg/Ca at time t (i.e., Eocene, subscript t) and today (subscript 0), A and B are the exponential and pre-exponential constants respectively, and T is temperature (Lear et al., 2002). The temperatures from Eocene foraminifera were calculated using a multi-species Mg/Ca-temperature calibration for modern tropical and sub-tropical planktonic foraminifera ($A = 0.09$, $B = 0.38$; Anand et al., 2003), and a calibration from three modern *Cibicidoides* species for benthic foraminifera ($A = 0.109$, $B = 0.867$; Lear et al., 2002). Based on the uncertainties in these published calibrations, the propagated error in reconstructed temperatures is ca. ±1.5 °C for both planktonic and benthic species.

Secular changes in the Mg/Ca ratio of seawater (Mg/Ca_{sw}) have occurred over timescales of millions of years, and various models and proxies have estimated Mg/Ca_{sw} through time (Billups and Schrag, 2003; Coggon et al., 2010; Dickson, 2002; Hardie, 1996; Lear et al., 2002; Lowenstein et al., 2001, 2003; Stanley and Hardie, 1998; Wilkinson and Algeo, 1989; Zimmermann, 2000). Given that Eocene seawater is likely to have had lower Mg/Ca than the present day, we calculated sea temperatures using a conservative estimate of Eocene seawater Mg/Ca of 3.35 mmol/mol, or 35% lower than the present day (Lear et al., 2002), although other estimates do predict lower values. An even lower Mg/Ca ratio for Eocene seawater has the effect of increasing calculated Mg/Ca sea temperatures, and thus we consider all our presented temperature estimates are minimum values.

4. Results

4.1. Trace element/Ca analysis of mid-Waipara foraminifera

A preliminary study of the Eocene foraminifera found at mid-Waipara involved the characterization of all the different species present to select a subset of species for use in the detailed temperature–time record. In this initial study, every specimen present in three samples (MW106, MW112, and MW118) with the widest assemblage of species was analysed. A total of 13 different species were analysed, and showed significant differences in typical trace element profiles, inter- and intra-test variability, and trace element chemistry between these Eocene taxa (see Supplementary information). On the basis of the data obtained in this preliminary investigation, 5 species characterized by the least disturbed trace element depth profiles and most consistent data (*M. crater*, *A. primitiva*, *C.* sp. A, *B. subbortonica*, and *V. marshalli*) were selected for analysis through the entire mid-Waipara section.

The five selected species analysed from all of the mid-Waipara samples, cover the period 50.7 to 46.5 Ma at a temporal resolution of 100 to 300 kyr (Table S1). Both the abundance of foraminifera and their degree of preservation decrease upward through the section. Planktonic species were generally found to yield poorer analyses than benthics with only *ca.* 30% of the total analyses for each of the planktonic species passing the screening process, compared with *ca.* 70% for the benthic species. The decrease in preservation towards the top of the section is often reflected by extreme trace element/Ca ratios, which has resulted in more analyses being rejected, and many of the samples from the upper part of the section yield few, if any, useable analyses from planktonic species. The preservation has had a lesser effect on the quality of the benthic trace element data, even at the top of the section where only the most diagenetically affected samples had <50% of the analyses passing screening.

Al/Ca ratios were generally observed to increase up-section in all species, accompanying the decrease in preservation. However, the screening process effectively removes any effect on calculated Mg/Ca paleo-sea temperatures as no significant correlation between Al/Ca and Mg/Ca amongst the individual analyses of any species from a particular sample is observed. Sr/Ca ratios are essentially uniform throughout the record within each species, although there appear to be subtle systematic differences in Sr/Ca ratios between different species. For example, while most of the species have average Sr/Ca = 1.1 to 1.3 mmol/mol, *V. marshalli* exhibits higher Sr/Ca of *ca.* 1.6 mmol/mol, which accompanies its systematically higher Mg/Ca as compared to the other benthic species. All species show a marked decrease (60–90%) in Mn/Ca towards the top of the section. While most trace element depth profiles (e.g., Fig. 3) show a Mn/Ca enrichment at the surface, in most analyses for the remainder of the depth profile, Mn/Ca is relatively constant and Mn/Ca ratios are also consistent between individuals within each sample.

For most samples, Mg/Ca-temperatures from the three benthic species (*C.* sp. A, *B. subbortonica* and *V. marshalli*) are within *ca.* 2.5 °C of each other, although for several samples they differ by up to *ca.* 4 °C. The disparity between the three benthic temperature series is greatest at the top of the section where the data is poorest. However, these temperatures are still mostly within error of one another. The 95% confidence intervals (based on intra-sample variability) in the benthic Mg/Ca temperature data are typically on the order of 0.5–1.5 °C, although these are significantly higher for samples that had very few analyses.

4.2. Changes in Mg/Ca paleo-sea temperatures through the mid-Waipara section

Smoothed records for SST and BWT were calculated from weighted means of the Mg/Ca temperatures from planktonic and benthic foraminifera taxa, respectively. Weightings are based on 95% confidence intervals (CI) for each temperature data point (i.e. intra-sample variability). Temperatures that are based on a single analysis (i.e. have no standard deviation) were given a low, but not zero, weighting. Data points that end up with artificially large confidence intervals solely from the small number of analyses, (i.e. have a similar standard deviation but a large t-distribution (TINV)) were given fixed confidence intervals of 6 °C. The smoothed records are found to describe the data set well (Fig. 4, Table 1). Most of the residual temperatures for the planktonic data include zero in their error bars, and the same is true for almost all of the benthic residual temperatures.

Planktonic foraminiferal Mg/Ca ratios range from *ca.* 3.6 mmol/mol at the bottom of the section to *ca.* 2.0 mmol/mol at the top of the section, indicating a general cooling from *ca.* 30 °C to 23 °C. Temperatures are relatively stable for the first half of the record yielding 27–30 °C from planktonic species and 18–21 °C from benthic species, with the exception of two samples (MW100 and MW103), which are cooler by *ca.* 4 °C for planktonic species and 2–3 °C for benthic species. In sample MW115 (49.0 Ma), *M. crater* yields a slightly cooler temperature that may represent a subtle cooling that is not observed in the benthic record. The second half of the record is dominated by a cooling trend from *ca.* 48.7 Ma, observed in both SST and BWT.

In general, the Mg/Ca SST and BWT records show strong agreement. An overall trend of cooling is observed in both the SST and BWT records. Temperatures during the first half of the record (*ca.* 51–48.7 Ma) were relatively stable, with most of the observed cooling taking place from *ca.* 48.7 Ma onwards. A transient cooling event is observed in SST and BWT between *ca.* 50.5 and 50.0 Ma, with a *ca.* 4 °C decrease in SST, and a slightly subdued cooling of 2–3 °C in the BWT record. However, the broad cooling over the entire record is approximately equal in magnitude (*ca.* 5–6 °C) in both the SST and BWT records.

5. Discussion

5.1. Do the Mg/Ca temperatures reliably record past sea temperatures?

The three different temperature proxy records (Mg/Ca, TEX_{86}, and $\delta^{18}O$) available from mid-Waipara all yield very warm temperatures for the Early Eocene and a general cooling trend over the length of the record (Fig. 4). The three SST proxies yield similar temperatures in the range of 25–35 °C, and the two benthic records are in the range of 15–25 °C. The proxy records show common temporal variations, but these vary in magnitude between different proxies. While there is good agreement between the Mg/Ca and TEX_{86} SSTs, which is discussed further in Section 5.2, the oxygen isotope records are slightly more complicated. The planktonic $\delta^{18}O$ temperature record has roughly the same mean value as the planktonic Mg/Ca and TEX_{86} temperature records and shows very similar trends. However, the $\delta^{18}O$ SST changes are significantly larger than those recorded by Mg/Ca ratios or TEX_{86} data (Fig. 4). The benthic $\delta^{18}O$ record also records these amplified changes in temperatures as compared to the other proxies. The reasons for this are considered further in Section 5.3.

Figure 5 shows several of the various proxy records normalized to their standard deviations (i.e. mean subtracted and variability scaled to number of standard deviations from the mean). These normalized records give a clear picture of the temperature trends over time, and illustrate that the temperature variability is very consistent between the proxy records. Of the two planktonic Mg/Ca records, *M. crater* shows a much better agreement with the other records than the smoothed SST record (*M. crater* + *A. primitiva*), and the *M. crater* Mg/Ca record is the preferred Mg/Ca SST record obtained in this study. The correlation between these records gives clear evidence that the three independent proxies are all recording a common (temperature) signal.

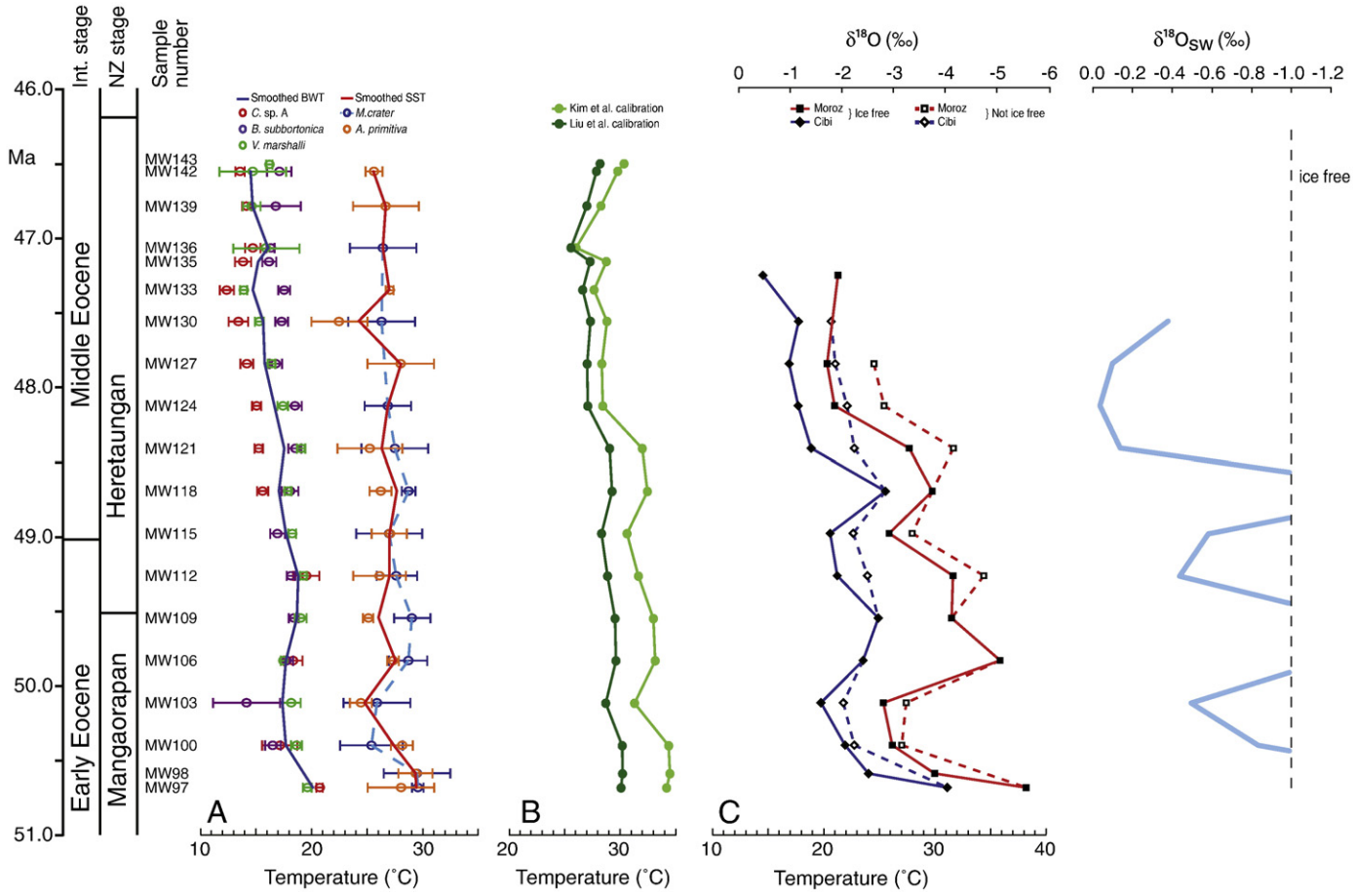

Fig. 4. Paleo-sea temperature data from the mid-Waipara section. A) Mg/Ca-temperatures from mid-Waipara for 5 species of foraminifera. Blue circles = *M. crater*; orange circles = *A. primitiva*; red circles = *C.* sp. A; purple circles = *B. subbortonica*; green circles = *V. marshalli*. Error bars on the data are 95% confidence intervals based on the range of temperatures that were used to calculate the average temperature from each species for each sample. Solid lines are smoothed SST (red) and BWT (blue) records, which are weighted means of the Mg/Ca data at each point from 95% confidence intervals. The *M. crater* Mg/Ca record shows much better agreement with other SST proxies than the smoothed SST from *M. crater and A. primitiva*, thus the *M. crater* record (dashed blue line) is our preferred Mg/Ca SST record. B) TEX_{86} sea surface temperature data from Hollis et al. (2009) calculated using two different calibrations. The dark green line is the non-linear calibration of Liu et al. (2009), whereas the light green line is the linear calibration of Kim et al. (2008). C) Oxygen isotope data and calculated calcification temperatures. Red lines are the temperature record from planktonic foraminifera (*Morozovella*) and blue lines are the temperature record from benthic foraminifera (*Cibicides*). Solid lines are calculated with a fixed $\delta^{18}O_{sw}$ of −1‰ (Zachos et al., 1994). Dashed lines are calculated using the $\delta^{18}O_{sw}$ in (d). D) $\delta^{18}O_{sw}$ back-calculated from benthic foraminiferal $\delta^{18}O$ and Mg/Ca temperatures, as described in the text and Supplementary information.

As a means of quantifying how well the different proxies agree, the smoothed benthic Mg/Ca-temperature record was treated as a "model" temperature. Residual (proxy–model) temperatures were calculated for each of the other proxies after correcting for mean offsets. For example, if the TEX_{86} temperature record (using the Liu et al. calibration) had the same mean as the smoothed benthic record, the average difference (=mean residual) between the two records would be just 0.8 °C. Using the Kim et al. (2008) calibration the mean residual would be 1.3 °C. Thus, TEX_{86} temperatures from both calibrations show a strong agreement with Mg/Ca temperatures. The oxygen isotope temperature residuals are much larger, as expected given the much larger amplitudes of the variations in the data, with mean residuals of 3.7 °C for the planktonic $\delta^{18}O$ temperatures, and 2.5 °C for the benthic $\delta^{18}O$ temperatures.

The strong agreement between the Mg/Ca paleo-sea temperatures and two independent temperature proxies indicates that the laser ablation ICP-MS technique is effective in extracting reliable and meaningful temperatures even from what are, in some cases, relatively poorly preserved specimens. The similarity in the magnitude of reconstructed SST and BWT proxy records also suggest that the Mg/Ca-temperature calibrations from modern species appear to be applicable to Eocene species of foraminifera.

5.2. Implications for the seawater Mg/Ca ratio in the Eocene ocean

The Mg/Ca value for Eocene seawater used in this study to calculate sea temperatures (3.35 mmol/mol) is a conservative value, and while Lear et al. (2002) argue that it is unlikely that Mg/Ca_{sw} would have been less than 3.35 mmol/mol, published estimates from other models and proxies extend to values as low as 1.5–2.0 mmol/mol (Dickson, 2002; Hardie, 1996; Lowenstein et al., 2001; Stanley and Hardie, 1998), which would raise Mg/Ca sea temperatures by up to 10 °C as compared to the values shown here (Tables 1, S1 and S2; Fig. 4A).

TEX_{86} SSTs are independent of the seawater Mg/Ca ratio, and these can thus be used to constrain the Mg/Ca values of seawater during the Eocene, including any potential significant changes over time (assuming that the Mg/Ca-temperature calibration is accurate for these Eocene foraminifera). However, comparison between Mg/Ca and TEX_{86} SSTs is complicated by disagreement over temperature calibrations for TEX_{86}. While there is good agreement between Mg/Ca and TEX_{86} SSTs in terms of the timing and magnitude of temperature variations, the absolute TEX_{86} SST values depend on which calibration is used (Fig. 4B).

An Eocene Mg/Ca_{sw} of 3.35 mmol/mol (Lear et al., 2003), fixed throughout the duration of the record, results in a very close match

Table 1
Reconstructed Mg/Ca paleo-sea temperatures for the full suite of mid-Waipara samples, including smoothed SST and BWT records generated from Mg/Ca data, and comparative $\delta^{18}O$ and TEX_{86} temperatures from the same samples (Hollis et al., 2009). Temperatures from TEX_{86} are calculated from two different calibrations (Kim et al., 2008; Liu et al., 2009), which yield somewhat different temperatures. $\delta^{18}O$ temperatures are calculated using a fixed $\delta^{18}O_{sw}$ for an assumed ice-free world ($\delta^{18}O_{sw} = -1‰$) and using calculated $\delta^{18}O_{sw}$ reconstructed from Mg/Ca temperature data, which allows for the presence of continental ice in the greenhouse.

Sample number	Age (Ma)	Mg/Ca temperatures							TEX_{86} SST		$\delta^{18}O$ (ice-free)		$\delta^{18}O$ (with ice)	
		M. crater	*A. primitiva*	Smoothed SST	*C. sp. A*	*B. subbortonica*	*V. marshalli*	Smoothed BWT	Kim et al. (2008) calibration	Liu et al. (2009) calibration	SST (*Morozovella*)	BWT (*Cibicides*)	SST (*Morozovella*)	BWT (*Cibicides*)
MW143	46.5						16.0							
MW142	46.6		25.6	25.6	13.5	17.3	14.7	14.5	29.8	27.8				
MW139	46.8	23.3	27.0	26.7	14.1	16.1	13.9	14.7	28.2	27.0				
MW136	47.1	26.4		26.4	14.7	16.2	15.9	16.1	26.0	25.5				
MW135	47.2				13.8	16.0		15.1	28.7	27.2				
MW134	47.2										21.2	14.5		
MW133	47.3		27.1	27.0	12.9	17.5	13.6	14.7	27.6	26.6				
MW130	47.6	26.3	22.8	24.2	13.4	17.3	15.3	15.6	28.8	27.3		17.7		20.5
MW127	47.8		30.6	28.0	14.2	16.8	16.2	15.8	28.3	27.0	20.3	16.8	24.4	21.0
MW124	48.1	27.7		26.9	15.0	18.2	17.4	16.7	28.4	27.1	20.9	17.7	25.4	22.1
MW121	48.4	27.8	25.2	26.3	15.2	18.0	18.9	17.5	32.0	29.0	27.6	18.8	31.6	22.8
MW118	48.7	28.8	26.2	27.7	15.9	18.0	17.8	17.1	32.5	29.3	29.6	25.4	29.6	25.4
MW115	49.0	27.3	27.2	27.0		16.9	18.2	17.7	30.6	28.3	25.8	20.5	27.7	22.4
MW112	49.3	28.2	26.7	27.0	19.5	18.1	19.2	18.8	31.6	28.8	31.5	21.2	34.2	23.8
MW109	49.5	29.3	25.0	26.0		18.4	19.0	18.6	33.0	29.5	31.4	24.8	31.4	24.8
MW106	49.8	29.5	27.5	27.6	18.3	17.8	17.4	17.6	33.2	29.6	35.7	23.4	35.7	23.4
MW103	50.1	25.8	24.4	24.8		14.1	17.7	17.3	31.3	28.7	25.3	19.7	27.6	22.0
MW100	50.4	25.4	28.7	27.4	17.1	16.5	18.6	17.6	34.4	30.2	26.1	21.9	26.8	22.6
MW98	50.6	29.4	29.3	29.4					34.5	30.2	29.8	23.9		
MW97	50.7	29.6	28.0	29.3	20.7		19.6	20.2	34.2	30.1	38.0	31.0	38.0	31.0

Note: As the temperatures from *M. crater* show a much better agreement with the other records than the smoothed planktonic record (*M. crater* + *A. primitiva*), and the planktonic $\delta^{18}O$ is also based on *Morozovella*, the *M. crater* Mg/Ca record is the preferred Mg/Ca SST record.

between planktonic Mg/Ca and TEX_{86} SSTs using the non-linear calibration of Liu et al. (2009). If the Liu et al. (2009) calibration is correct, this suggests that this Mg/Ca_{sw} is close to the true value. However, using the calibration of Kim et al. (2008), TEX_{86} temperature estimates are higher by up to 4.5 °C and show a greater cooling over the time interval, potentially implying our assumed Mg/Ca_{sw} is too conservative (i.e., high) and that Mg/Ca_{sw} has changed over the duration of the record. By adjusting the planktonic Mg/Ca SST data to match the TEX_{86} record, it is possible to estimate the required Mg/Ca_{sw} and its rate of change. Doing so requires Mg/Ca_{sw} to be 2.24 mmol/mol at the bottom of the record increasing to 3.04 mmol/mol by the top of the record (assuming the change in Mg/Ca_{sw} to be linear), and results in a good fit between SSTs derived from Mg/Ca and TEX_{86} calculated with the Kim et al. (2008) calibration. Applying the same Mg/Ca_{sw} values to the benthic Mg/Ca data also increases BWT estimates, and improves the agreement between the benthic Mg/Ca and $\delta^{18}O$ records. However, the implied rate of change in Mg/Ca_{sw} of 0.19 mmol/mol per Myr is significantly steeper than modelled estimates, which predict a maximum rate of *ca.* 0.08 mmol/mol per Myr (Stanley and Hardie, 1998; Wilkinson and Algeo, 1989).

A comparison of Mg/Ca and TEX_{86} SSTs indicates that the Mg/Ca ratio of Eocene seawater is unlikely to have been lower than 2 mmol/mol because lower estimates of seawater Mg/Ca increase reconstructed Mg/Ca paleo-sea temperatures beyond the range suggested by two independent temperature proxies. Recently, Coggon et al. (2010) published a record of Mesozoic and Cenozoic seawater Mg/Ca and Sr/Ca ratios extending back to *ca.* 170 Ma based on trace element concentrations from mid-ocean ridge flank calcium carbonate veins. The estimates from Coggon et al. (2010) of Paleogene seawater Mg/Ca range from 1.2 to 2.5 mmol/mol. The sensitivity of the Mg/Ca paleothermometer to changes in the Mg/Ca ratio of seawater is shown in Figure 6. Based on our Mg/Ca data, seawater Mg/Ca ratios of <1.5 mmol/mol have the effect of increasing reconstructed Mg/Ca temperatures by 7.5–11.5 °C (Fig. 6), resulting in temperatures that seem implausibly high (36–41 °C), especially considering temperatures from TEX_{86}. Additionally, seawater Sr/Ca ratios from Coggon et al. (2010) are estimated at $Sr/Ca = 2.8 \pm 1$ mmol/mol (i.e. 3 times lower than the present day). By inverting the Sr/Ca partition coefficient between seawater and foraminiferal calcite from Lear et al. (2003) ($D_{Sr} = 0.165$), the Eocene seawater Sr/Ca of Coggon et al. (2010) should be reflected by foraminiferal Sr/Ca ratios of 0.3–0.6 mmol/mol. Foraminiferal Sr/Ca ratios measured in this study are generally in the range of 1.0–1.4 mmol/mol, which is consistent with observations in previous trace element studies of Eocene foraminifera (Lear et al., 2003; Tripati et al., 2003), and thus the results of this study are inconsistent with the Eocene seawater Sr/Ca and Mg/Ca reconstructions of Coggon et al. (2010).

5.3. Comparison with oxygen isotope data

The oxygen isotope temperature record from the Ashley Mudstone is observed to vary sympathetically with temperatures derived from Mg/Ca and TEX_{86} throughout the studied interval. However, the $\delta^{18}O$-temperature record exhibits larger amplitude fluctuations than the other temperature proxies (Fig. 4). These fluctuations are observed in both the planktonic and benthic $\delta^{18}O$ records, and it is therefore unlikely that local evaporation and salinity effects are responsible for the amplified temperature changes. An explanation for this increase in amplitude requires a mechanism that can amplify both positive and negative $\delta^{18}O$ excursions while preserving the primary trend in temperature.

A diagenetic explanation requires that post-depositional diagenetic processes were acting to different degrees over the record, i.e. that foraminifera deposited during warm intervals were better preserved (less diagenetically altered) than those deposited during cooler intervals. This could occur as a result of the deposition of more clay-rich sediment during warmer periods, which would lead to better preservation of foraminifera, while foraminifera deposited in cooler periods would be more susceptible to diagenesis. As diagenetic effects generally have the effect of lowering $\delta^{18}O$ temperatures, this would amplify the cooling signal.

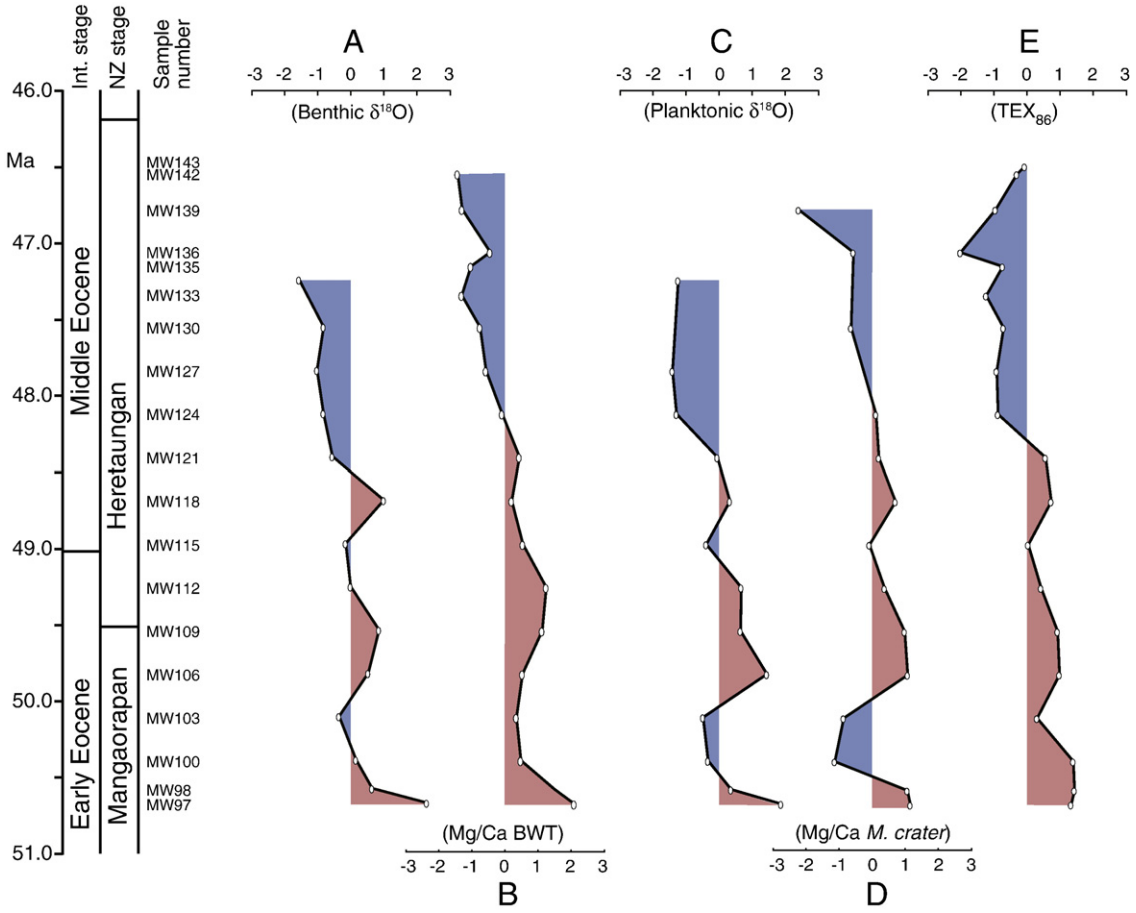

Fig. 5. Mid-Waipara proxy data, showing the agreement between the different temperature records available for this locality in the Eocene. Each record has had the mean subtracted, and variability has been scaled to the number of standard deviations from the mean. The normalized records display the relative temperature trends and the similarity between all the records irrespective of the type of proxy used to track sea temperatures. The excellent agreement between these independent records gives confidence that the LA-ICP-MS technique can extract reliable sea temperatures in foraminifera from these samples. (A) and (B) are BWT records from $\delta^{18}O$ and Mg/Ca, respectively; (C), (D) and (E) are SST records from $\delta^{18}O$, Mg/Ca and TEX_{86}, respectively.

Another mechanism that could amplify the $\delta^{18}O$-temperature signal without overprinting it and maintain synchronous variations between the three temperature proxies would be if $\delta^{18}O$ of seawater varied during this time interval (i.e. in response to the waxing and waning of continental ice sheets). In oxygen isotope temperature reconstructions, the Early Eocene Earth is often considered to have been free of significant continental ice, and temperatures are calculated assuming an "ice-free world" seawater $\delta^{18}O$ value. However, if small ephemeral ice sheets were forming and collapsing in polar regions during this time, a signal should be preserved in the $\delta^{18}O$ record. Given increasing evidence for polar ice sheets in the Eocene (e.g. Miller et al., 2005a; Peters et al., 2010; Tripati et al., 2005), it is possible that some of the high amplitude variation in $\delta^{18}O$ observed in the mid-Waipara section reflects changes in seawater $\delta^{18}O$ as a consequence of waxing and waning Eocene ice sheets. Using an independent record of temperature (such as Mg/Ca), the temperature component can be subtracted from the $\delta^{18}O$ record, yielding the $\delta^{18}O$ of seawater (e.g. Lear et al., 2000; Supplementary information). The $\delta^{18}O_{sw}$ calculated in this way is shown in Figure 4D and the effect on the $\delta^{18}O$ temperature record can be seen in Figure 4C. Allowing the $\delta^{18}O_{sw}$ to change in this way improves the match between $\delta^{18}O$ and the other proxies.

Conversion of these changes in $\delta^{18}O_{sw}$ to an approximate ice volume is difficult as it depends on the isotopic composition of ice sheets that would have existed in the Eocene, and the calibration of oxygen isotopes to ice volume. Sea level change estimates based on back stripping have shown pre-Oligocene changes in sea level on the order of several tens of metres (e.g. Browning et al., 2008; Haq et al., 1987; Kominz et al., 1998, 2008; Miller et al., 2003, 2005b; Müller et al., 2008; Pekar et al., 2005), which have been interpreted as too large and rapid to result from any other process than glacioeustacy (Miller et al., 2005a). At the temporal resolution and length of our record it is not possible to convincingly match the reconstructed Eocene $\delta^{18}O_{sw}$ with these sea level records (as per Billups and Schrag, 2002). However, the observed fluctuations in sea level do allow for the possibility of ice sheets during this period.

The presence of significant ice sheets in the earlier Eocene remains the subject of ongoing debate. Our record shows the possibility of some ice volume influence on the $\delta^{18}O$ of carbonates. However, it is more probable that the observed amplification of $\delta^{18}O$ temperatures arises from diagenetic effects. Further high-resolution multiproxy studies of early Paleogene records, including *in situ* analysis of different proxies in individual microfossils, may help to resolve this debate.

5.4. Cenozoic changes in the redox state of the ocean revealed through foraminiferal Mn/Ca ratios?

The manganese content of foraminifera is generally thought to reflect secondary diagenetic processes occurring on the sea-floor, and the precipitation of Mn carbonate and oxyhydroxide phases at the sediment–water interface (Boyle, 1983; Lea et al., 1999; Pingitore

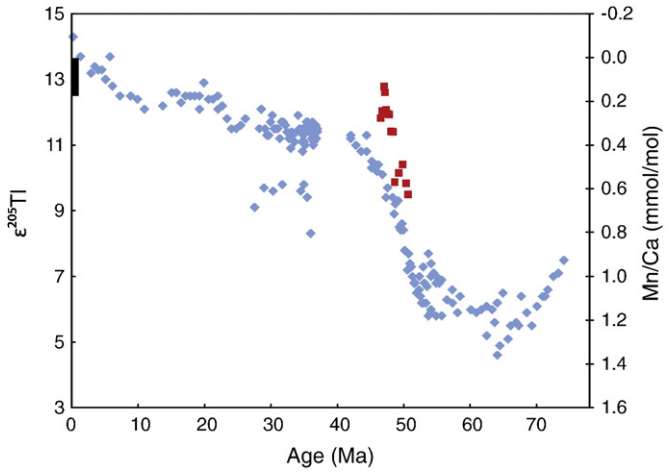

Fig. 6. Mn/Ca data from mid-Waipara (red squares; this study). The range of Mn/Ca ratios found in modern foraminifera analysed by similar LA-ICP-MS techniques (black rectangle; Marr, 2009) is also shown, and these are superimposed on thallium isotope data (blue diamonds) from Nielsen et al. (2009). The dramatic change in ε^{205}Tl from 55 to 45 Ma was interpreted by Nielsen et al. to reflect four times greater sequestration of Fe and Mn in the ocean by biological utilization. Mn/Ca data for the Cenozoic appears to support this hypothesis, with the major change in Mn/Ca occurring over the same period, which is covered by the mid-Waipara record. In the mid-Waipara data, Mn/Ca ratios decrease by 60–90% between 55 and 45 Ma.

et al., 1988) or in the sediment column (Wei et al., 2009). These phases are important in redox reactions in suboxic environments (Pingitore et al., 1988), and thus Mn/Ca ratios are significantly higher in reducing sediments, where remobilised Mn and Fe are precipitated as oxides or oxyhydroxides (Boyle, 1983). The deposition of authigenic Fe–Mn-oxyhydroxide phases in the ocean is largely controlled by redox conditions, which in turn depend on the amount of organic carbon deposition.

In mid-Waipara samples, mean benthic and planktonic foraminiferal Mn/Ca values show a decrease of 60–90% (e.g. Mn/Ca = *ca.* 0.5–0.08 mmol/mol) over the period 51–46 Ma. The interpretation of this is not entirely straightforward. The change in Mn/Ca accompanies a change in foraminifer preservation up-section. However, preservation is observed to decrease up-section. If the preservation also reflects the level to which those foraminifera were prone to diagenesis (which is inferred to be the case from laser ablation data), then logically one might expect the opposite trend in Mn/Ca (i.e. an increase up-section). While this observation does not preclude Mn-rich coatings as the source of Mn/Ca ratios, an alternative hypothesis could be that Mn/Ca is a primary feature, where Mn^{2+} has been incorporated into the calcite lattice during the precipitation of the foraminifera test. While Mn is present throughout laser ablation depth profiles (Fig. 3), which would be consistent with Mn/Ca being a primary feature, the same is also true of Al/Ca, which is inferred to be present from sediment infilling pore spaces. Thus, it is not possible to say with absolute confidence whether Mn/Ca ratios here reflect the presence of Mn-rich coatings occupying pore spaces, or whether it is a primary signal and thus might record the chemistry of the water column in which these foraminifera were living.

If Mn-rich coatings are responsible for Mn/Ca compositions, we can place some constraints on their chemistry. A weak correlation is observed between Mn/Ca and Mg/Ca (Table S3). However, linear regressions through Mg/Ca versus Mn/Ca data from the different species all have very low slopes, and do not converge towards a common end member. This means that if a mixed Ca–Mn–Mg carbonate phase (e.g. Boyle, 1983; Pena et al., 2005; Weldeab et al., 2006) was the contributor of Mn, they do not appear to have caused any significant bias to Mg/Ca temperatures. If, rather, manganese oxyhydroxide coatings were the source of Mn, the weak correlation observed between Mg/Ca and Mn/Ca may be merely a coincidence, whereby a cooling of sea temperatures directly caused a decrease in foraminifera Mg/Ca ratios, and indirectly caused a reduction in Mn/Ca ratios via an accompanying change in ocean redox conditions.

Regarding the implications for the redox conditions of the local basin, a decrease in the precipitation of Mn-rich contaminant phases would be expected to indicate a shift to a more oxidizing environment, i.e. a decrease in the burial of organic matter. However, this is inconsistent with a shift in carbon isotopes in planktonic foraminifera towards more positive values (Hollis et al., 2009), which indicates an increase in the export of marine organic matter from the surface ocean over the same period. An alternative explanation may come from a study of thallium (Tl) isotopes in ferromanganese crusts for the last ca. 74 Ma (Nielsen et al., 2009), which has shown that the rate of precipitation of authigenic Fe–Mn oxyhydroxides was several times higher in the Paleocene than for the remainder of the Cenozoic, and that most of the change between the two regimes occurred over the period 55–45 Ma (i.e. the same time period covered by the mid-Waipara record). Mn/Ca data from mid-Waipara and another LA-ICP-MS data set from modern foraminifera specimens (Marr, 2009) are shown overlain on the ε^{205}Tl data of Nielsen et al. (2009) (Fig. 7). Nielsen et al. attribute the reduced sequestration of Tl by Fe–Mn oxyhydroxides to greatly increased biological utilization of Fe and Mn and increased marine organic carbon burial since the Paleocene.

Thus, the decrease in the Mn/Ca content of foraminifera over the mid-Waipara record may reflect reduction in the precipitation of

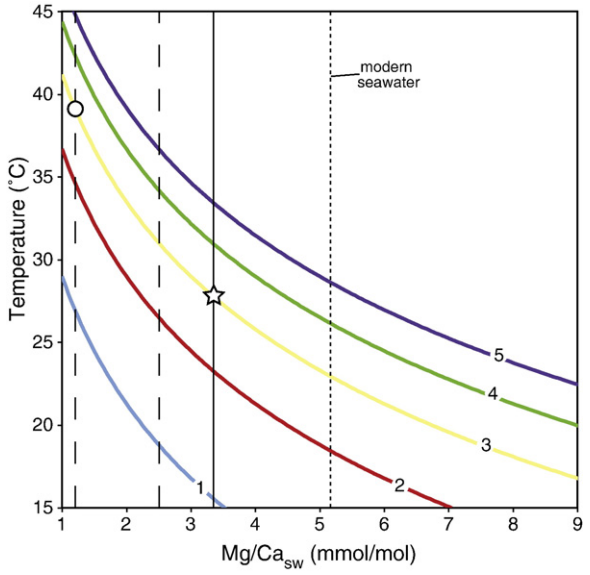

Fig. 7. Graphical illustration of the sensitivity of temperature reconstructions to seawater Mg/Ca ratios. The contours represent planktonic foraminiferal Mg/Ca ratios in mmol/mol, converted to temperature using the planktonic calibration of Anand et al. (2003). The vertical lines represent seawater Mg/Ca values: dotted black line = Modern seawater Mg/Ca (Lear et al., 2003); solid black line = Lear et al. (2003) estimate of minimum Eocene seawater Mg/Ca (=3.35 mmol/mol), which was used for the calculation of temperatures in this study; dashed black lines = upper and lower limit of seawater Mg/Ca for the period 170–24 Ma from Coggon et al. (2010). The open star represents the intersection between the mean Mg/Ca ratio of the planktonic foraminifera species *M. crater* from mid-Waipara and the assumed Mg/Ca_{sw} from Lear et al. (2003). The open circle represents the maximum temperature estimate based on the intersection between the mean Mg/Ca ratio of the planktonic foraminifera species *M. crater* from mid-Waipara and the lower estimate of Mg/Ca_{sw} from Coggon et al. (2010). Thus, for the measured Mg/Ca ratios at mid-Waipara, using a seawater Mg/Ca value of 1.2 mmol/mol increases Mg/Ca SST estimates by ca. 11.5 °C as compared to using the assumed value of 3.35 mmol/mol, yielding sea surface temperatures of ca. 35–40 °C. For benthic foraminifera, a seawater Mg/Ca ratio of 1.2 mmol/mol increases temperatures by 9–10 °C above those calculated using the assumed value of 3.35 mmol/mol, yielding bottom water temperatures of 23–30 °C.

manganese carbonate and oxyhydroxide coatings caused by the reduced availability of Fe–Mn in seawater, brought about by increased ocean productivity, which is consistent with the observed cooling. This is also consistent with the increased organic matter burial indicated by carbon isotopes (Hollis et al., 2009). Such an argument may satisfy either possibility for the source of Mn — a reduction in the availability of Mn in seawater would limit the availability for both precipitation from the water column, or for the formation of Mn-oxyhydroxide coatings. This interpretation is tenuous, however, given that the substitution of Mn into foraminiferal calcite is not well understood, and additionally the residence time of Mn in the ocean is short and thus changes in Mn/Ca may not reflect global processes. However given the consistency between modern foraminiferal Mn/Ca data (Marr, 2009), Eocene foraminiferal Mn/Ca data from mid-Waipara (this study), and the thallium isotope data of Nielsen et al. (2009) for the same period, there appears to be grounds for a common interpretation.

5.5. Implications for global climate

Three independent geochemical proxies yield tropical sea temperatures for New Zealand's Canterbury Basin during the Early Eocene with SSTs of 26–30 °C and BWTs of 16–20 °C in the bathyal setting at mid-Waipara. These temperatures are similar to other published SST estimates from lower latitude deep-sea cores for the Early to Middle Eocene (Sexton et al., 2006; Tripati et al., 2003) and from the Paleocene–Eocene thermal maximum (Zachos et al., 2006). Some significant climate events are common to all of these proxy records, which are highlighted by the normalized records in Figure 5. A transient event is observed in SST and BWT in all proxy records between *ca.* 50.5 and 50.0 Ma, with a cooling of *ca.* 4 °C in sea surface temperatures. Given the amplified oxygen isotope signal, the cooling in BWT was probably closer to the 2–3 °C indicated by the Mg/Ca BWT record. This cooling took place over *ca.* 0.6 Myr, reaching a local minimum at around 50.2 Ma. While this transient cooling of *ca.* 4 °C at mid-Waipara may not reflect a global cooling of that magnitude, the fact that it affected both sea surface and bottom water temperatures means that it is unlikely to be a localized phenomenon, and this cooling could represent a global climate event.

A cooling trend is observed from *ca.* 48.7 Ma onwards in reconstructed temperatures from all three of the temperature proxies. We interpret this final cooling event as the termination of the EECO for the southern mid-latitudes, and the beginning of the greenhouse to icehouse transition. By 46.5 Ma, SSTs drop to below *ca.* 24 °C and BWTs to below 15 °C.

The timing of the termination of the EECO at mid-Waipara (*ca.* 48.7 Ma) is consistent with an 800 kyr interval at ~48.5 Ma where the freshwater *Azolla* fern is thought to have grown in large quantities in freshened surface waters of the geographically restricted Eocene Arctic Ocean (Brinkhuis et al., 2006). Thus, the temperature records presented here support the hypothesis that the rapid growth of the *Azolla* fern may have drawn down significant amounts of atmospheric CO_2 triggering the transition to the icehouse world (Brinkhuis et al., 2006; Speelman et al., 2009).

6. Conclusions

A LA-ICP-MS study of the trace element chemistry of Eocene (51–46 Ma) planktonic and benthic foraminifera from mid-Waipara, southern New Zealand has shown that:

(1) This technique can extract reliable Mg/Ca paleo-sea temperature data from Eocene foraminifera, even from moderately poorly preserved specimens, as demonstrated by agreement with sea surface and bottom water temperature data from two independent proxies (TEX_{86} and $\delta^{18}O$).

(2) The agreement between proxies also indicates that the Mg/Ca-temperature calibrations from modern species appear to be applicable to Eocene foraminifera.

(3) During the EECO, sea surface temperatures at mid-Waipara (paleo-latitude *ca.* 55°S) were 28–30 °C, and bottom water temperatures were 18–20 °C. Temperatures were generally consistent for the period *ca.* 51–48.7 Ma with the exception of a 0.5 Myr transient cooling of 3–4 °C between *ca.* 50.5 and 50.0 Ma, and then sea temperatures steadily declined from *ca.* 48.7 Ma until the end of the record at 46.5 Ma. A net cooling of *ca.* 6 °C is observed over the entire mid-Waipara record.

(4) Reconstructed Mg/Ca paleo-sea temperatures show excellent agreement with TEX_{86} temperatures, which provides constraints on estimates of the Mg/Ca of Eocene seawater. The value of seawater Mg/Ca depends on the TEX_{86} temperature calibration used, but is in the range of 2.24–3.35 mmol/mol.

(5) An amplified temperature signal is observed in $\delta^{18}O$ relative to TEX_{86} and Mg/Ca in this record. While the oxygen isotope signal has almost certainly been disturbed to some extent by diagenesis, the $\delta^{18}O_{sw}$ record provides some evidence for the growth and collapse of ephemeral ice sheets on Antarctica during the Early Eocene greenhouse.

(6) The termination of the EECO and the beginning of the transition from greenhouse to icehouse conditions occurred at *ca.* 48.7 Ma, approximately concurrent with the “Azolla interval” in the Arctic Ocean, supporting the hypothesis that this event drew down significant amounts of atmospheric CO_2 and triggered the cooling that followed.

Acknowledgements

The authors would like to thank J. P. Marr for providing comparative trace element data, and M. Huber and R. D. Pancost for productive discussions in the preparation of this manuscript. We thank T. R. Naish and S. G. Nielsen for helpful comments on the manuscript. We also wish to thank three anonymous reviewers for their detailed and constructive comments.

Appendix A. Supplementary data

Supplementary data to this article can be found online at doi:10.1016/j.epsl.2010.09.039.

References

Anand, P., Elderfield, H., Conte, M.H., 2003. Calibration of Mg/Ca thermometry in planktonic foraminifera from a sediment trap time series. Paleoceanography 18, 1050.

Barker, S., Greaves, M., Elderfield, H., 2003. A study of cleaning procedures used for foraminiferal Mg/Ca paleothermometry. Geochem. Geophys. Geosyst. 4, 8407.

Berggren, W.A., Pearson, P.N., 2006. Taxonomy, biostratigraphy, and phylogeny of Eocene *Morozovella*. In: Pearson, P.N., Olsson, R.K., Huber, B.T., Hemleben, C., Berggren, W.A. (Eds.), Atlas of Eocene Planktonic Foraminifera: Cushman Foundation for Foraminiferal Research Special Publication, 41, pp. 343–376.

Berggren, W.A., Kent, D.V., Swisher III, C.C., Aubry, M.-P., 1995. A revised Cenozoic geochronology and chronostratigraphy. In: Berggren, W.A., Kent, D.V., Aubry, M.-P., Hardenbol, J. (Eds.), Geochronology, Time Scales and Global Stratigraphic Correlation: SEPM Special Publication, 54, pp. 129–212.

Berggren, W.A., Pearson, P.N., Huber, B., Wade, B.S., 2006. Taxonomy, biostratigraphy, and phylogeny of Eocene *Acarinina*. In: Pearson, P.N., Olsson, R.K., Huber, B.T., Hemleben, C., Berggren, W.A. (Eds.), Atlas of Eocene Planktonic Foraminifera: Cushman Foundation for Foraminiferal Research Special Publication, 41, pp. 257–326.

Bijl, P.K., Schouten, S., Sluijs, A., Reichart, G., Zachos, J.C., Brinkhuis, H., 2009. Early Palaeogene temperature evolution of the southwest Pacific Ocean. Nature 461, 776–779.

Billups, K., Schrag, D.P., 2002. Paleotemperatures and ice volume of the past 27 Myr revisited with paired Mg/Ca and $^{18}O/^{16}O$ measurements on benthic foraminifera. Paleoceanography 17, 1003.

Billups, K., Schrag, D., 2003. Application of benthic foraminiferal Mg/Ca ratios to questions of Cenozoic climate change. Earth Planet. Sci. Lett. 209, 181–195.

Boersma, A., Silva, I.P., Shackleton, N.J., 1987. Atlantic Eocene planktonic foraminiferal paleohydrographic indicators and stable isotope paleoceanography. Paleoceanography 2, 287–331.
Boyle, E.A., 1983. Manganese carbonate overgrowths on foraminifera tests. Geochim. Cosmochim. Acta 47, 1815–1819.
Brinkhuis, H., Schouten, S., Collinson, M.E., Sluijs, A., Damsté, J.S.S., Dickens, G.R., Huber, M., Cronin, T.M., Onodera, J., Takahashi, K., Bujak, J.P., Stein, R., van der Burgh, J., Eldrett, J.S., Harding, I.C., Lotter, A.F., Sangiorgi, F., Cittert, H.V.K., de Leeuw, J.W., Matthiessen, J., Backman, J., Moran, K., The Expedition 302 Scientists, 2006. Episodic fresh surface waters in the Eocene Arctic Ocean. Nature 441, 606–609.
Browning, J.V., Miller, K.G., Sugarman, P.J., Kominz, M.A., McLaughlin, P.P., Kulpecz, A.A., Feigenson, M.D., 2008. 100 Myr record of sequences, sedimentary facies and sea level change from Ocean Drilling Program onshore coreholes, US Mid-Atlantic coastal plain. Basin Res. 20, 227–248.
Burgess, C.E., Pearson, P.N., Lear, C.H., Morgans, H.E., Handley, L., Pancost, R.D., Schouten, S., 2008. Middle Eocene climate cyclicity in the southern Pacific: implications for global ice volume. Geology 36, 651–654.
Coggon, R.M., Teagle, D.A.H., Smith-Duque, C.E., Alt, J.C., Cooper, M.J., 2010. Reconstructing past seawater Mg/Ca and Sr/Ca from mid-ocean ridge flank calcium carbonate veins. Science 327, 1114–1117.
Cooper, R.A. (Ed.), 2004. The New Zealand Geological Timescale: Institute of Geological and Nuclear Sciences Monograph, 22. 284 pp.
Dickson, J.A.D., 2002. Fossil echinoderms as monitor of the Mg/Ca ratio of Phanerozoic oceans. Science 298, 1222–1224.
Eggins, S., De Deckker, P., Marshall, J., 2003. Mg/Ca variation in planktonic foraminifera tests: implications for reconstructing palaeo-seawater temperature and habitat migration. Earth Planet. Sci. Lett. 212, 291–306.
Eggins, S.M., Sadekov, A., De Deckker, P., 2004. Modulation and daily banding of Mg/Ca in *Orbulina universa* tests by symbiont photosynthesis and respiration: a complication for seawater thermometry? Earth Planet. Sci. Lett. 225, 411–419.
Erez, J., Luz, B., 1983. Experimental paleotemperature equation for planktonic foraminifera. Geochim. Cosmochim. Acta 47, 1025–1031.
Haq, B., Hardenbol, J., Vail, P., 1987. Chronology of fluctuating sea levels since the Triassic. Science 235, 1156–1167.
Hardie, L.A., 1996. Secular variation in seawater chemistry: an explanation for the coupled secular variation in the mineralogies of marine limestones and potash evaporites over the past 600 Myr. Geology 24, 279–283.
Hayward, B.W., Hollis, C.J., Grenfell, H.R., 1997. Recent *Elphidiidae* (Foraminferida) of the South-west Pacific and fossil *Elphidiidae* of New Zealand. Inst. Geol. Nucl. Sci. Monogr. 16, 1–170.
Hollis, C.J., Handley, L., Crouch, E.M., Morgans, H.E., Baker, J.A., Creech, J., Collins, K.S., Gibbs, S.J., Huber, M., Schouten, S., Zachos, J.C., Pancost, R.D., 2009. Tropical sea temperatures in the high-latitude South Pacific during the Eocene. Geology 37, 99–102.
Jenkins, D.G., 1971. New Zealand Cenozoic planktonic foraminifera. N.Z. Geol. Surv. Bull. 70 173 pp.
Jochum, K.P., Stoll, B., 2008. Reference materials for elemental and isotopic analyses by LA-(MC)-ICP-MS: successes and outstanding needs. In: Sylvester, P. (Ed.), Laser Ablation ICP-MS in the Earth Sciences: Current Practices and Outstanding Issues: Mineralogical Association of Canada Short Course, 40, pp. 147–168.
Kim, J., Schouten, S., Hopmans, E.C., Donner, B., Sinninghe Damsté, J.S., 2008. Global sediment core-top calibration of the TEX_{86} paleothermometer in the ocean. Geochim. Cosmochim. Acta 72, 1154–1173.
Kim, J., Meer, J.V.D., Schouten, S., Helmke, P., Willmott, V., Sangiorgi, F., Koç, N., Hopmans, E.C., Damsté, J.S.S., 2010. New indices and calibrations derived from the distribution of crenarchaeal isoprenoid tetraether lipids: implications for past sea surface temperature reconstructions. Geochim. Cosmochim. Acta 74, 4639–4654.
King, P.R., Naish, T.R., Browne, G.H., Field, B.D., Edbrooke, S.W., 1999. Cretaceous to recent sedimentary patterns in New Zealand. Inst. Geol. Nucl. Sci. Folio Ser. 1 35 pp.
Kominz, M.A., Miller, K.G., Browning, J.V., 1998. Long-term and short-term global Cenozoic sea-level estimates. Geology 26, 311.
Kominz, M.A., Browning, J.V., Miller, K.G., Sugarman, P.J., Mizintseva, S., Scotese, C.R., 2008. Late Cretaceous to Miocene sea-level estimates from the New Jersey and Delaware coastal plain coreholes: an error analysis. Basin Res. 20, 211–226.
Lea, D.W., Mashiotta, T.A., Spero, H.J., 1999. Controls on magnesium and strontium uptake in planktonic foraminifera determined by live culturing. Geochim. Cosmochim. Acta 63, 2369–2379.
Lear, C.H., Elderfield, H., Wilson, P.A., 2000. Cenozoic deep-sea temperatures and global ice volumes from Mg/Ca in benthic foraminiferal calcite. Science 287, 269–272.
Lear, C.H., Rosenthal, Y., Slowey, N., 2002. Benthic foraminiferal Mg/Ca-paleothermometry: a revised core-top calibration. Geochim. Cosmochim. Acta 66, 3375–3387.
Lear, C., Elderfield, H., Wilson, P., 2003. A Cenozoic seawater Sr/Ca record from benthic foraminiferal calcite and its application in determining global weathering fluxes. Earth Planet. Sci. Lett. 208, 69–84.
Lear, C.H., Bailey, T.R., Pearson, P.N., Coxall, H.K., Rosenthal, Y., 2008. Cooling and ice growth across the Eocene–Oligocene transition. Geology 36, 251–254.
Liu, Z., Pagani, M., Zinniker, D., DeConto, R., Huber, M., Brinkhuis, H., Shah, S.R., Leckie, R.M., Pearson, A., 2009. Global cooling during the Eocene–Oligocene climate transition. Science 323, 1187–1190.
Lowenstein, T.K., Timofeeff, M.N., Brennan, S.T., Hardie, L.A., Demicco, R.V., 2001. Oscillations in Phanerozoic seawater chemistry: evidence from fluid inclusions. Science 294, 1086–1088.
Lowenstein, T.K., Hardie, L.A., Timofeeff, M.N., Demicco, R.V., 2003. Secular variation in seawater chemistry and the origin of calcium chloride basinal brines. Geology 31, 857–860.
Marr, J. P., 2009. Ecological, oceanographic and temperature controls on the incorporation of trace elements into *Globigerina bulloides* and *Globoconella inflata* in the Southwest Pacific Ocean (M.Sc. thesis). Victoria University of Wellington.
Mashiotta, T.A., Lea, D.W., Spero, H.J., 1999. Glacial–interglacial changes in subantarctic sea surface temperature and $\delta^{18}O$-water using foraminiferal Mg. Earth Planet. Sci. Lett. 170, 417–432.
Miller, K.G., Sugarman, P.J., Browning, J.V., Kominz, M.A., Hernández, J.C., Olsson, R.K., Wright, J.D., Feigenson, M.D., van Sickel, W., 2003. Late Cretaceous chronology of large, rapid sea-level changes: Glacioeustasy during the greenhouse world. Geology 31, 585.
Miller, K.G., Wright, J.D., Browning, J.V., 2005a. Visions of ice sheets in a greenhouse world. Mar. Geol. 217, 215–231.
Miller, K.G., Kominz, M.A., Browning, J.V., Wright, J.D., Mountain, G.S., Katz, M.E., Sugarman, P.J., Cramer, B.S., Christie-Blick, N., Pekar, S.F., 2005b. The Phanerozoic record of global sea-level change. Science 310, 1293–1298.
Morgans, H.E.G., Jones, C.M., Crouch, E.M., Field, B.D., Hollis, C.J., Raine, J.I., Strong, C.P., Wilson, G.J., 2005. Upper Cretaceous to Eocene stratigraphy and sample collections, Mid-Waipara River section, North Canterbury. Institute of Geological and Nuclear Sciences Science Report 2003/08. 107 pp.
Müller, R.D., Bender, M., Gaina, C., Steinberger, B., Heine, C., 2008. Long-term sea-level fluctuations driven by ocean basin dynamics. Science 319, 1357–1362.
Nielsen, S.G., Mar-Gerrison, S., Gannoun, A., LaRowe, D., Klemm, V., Halliday, A.N., Burton, K.W., Hein, J.R., 2009. Thallium isotope evidence for a permanent increase in marine organic carbon export in the early Eocene. Earth Planet. Sci. Lett. 278, 297–307.
Pearce, N.J., Perkins, W.T., Westgate, J.A., Gorton, M.P., Jackson, S.E., Neal, C.R., Chenery, S.P., 1997. A compilation of new and published major and trace element data for NIST SRM 610 and NIST SRM 612 glass reference materials. Geostand. Geoanal. Res. 21, 115–144.
Pearson, P.N., Ditchfield, P.W., Singano, J., Harcourt-Brown, K.G., Nicholas, C.J., Olsson, R.K., Shackleton, N.J., Hall, M.A., 2001. Warm tropical sea surface temperatures in the Late Cretaceous and Eocene epochs. Nature 413, 481–487.
Pekar, S.F., Hucks, A., Fuller, M., Li, S., 2005. Glacioeustatic changes in the early and middle Eocene (51–42 Ma): shallow-water stratigraphy from ODP Leg 189 Site 1171 (South Tasman Rise) and deep-sea $\delta^{18}O$ records. Geol. Soc. Am. Bull. 117, 1081–1093.
Pena, L.D., Calvo, E., Cacho, I., Eggins, S., Pelejero, C., 2005. Identification and removal of Mn–Mg-rich contaminant phases on foraminiferal tests: implications for Mg/Ca past temperature reconstructions. Geochem. Geophys. Geosyst. 6 Q09P02.
Peters, S.E., Carlson, A.E., Kelly, D.C., Gingerich, P.D., 2010. Large-scale glaciation and deglaciation of Antarctica during the Late Eocene. Geology 38, 723–726.
Pingitore, N.E., Eastman, M.P., Sandidge, M., Oden, K., Freiha, B., 1988. The coprecipitation of manganese(II) with calcite: an experimental study. Mar. Chem. 25, 107–120.
Poore, R., Matthews, R., 1984. Oxygen isotope ranking of late Eocene and Oligocene planktonic foraminifers: implications for Oligocene sea-surface temperatures and global ice-volume. Mar. Micropaleontol. 9, 111–134.
Quilléveré, F., Norris, R.D., Moussa, I., Berggren, W.A., 2001. Role of photosymbiosis and biogeography in the diversification of early Paleogene *acarininids* (planktonic foraminifera). Paleobiology 27, 311–326.
Reichart, G., Jorissen, F., Anschutz, P., Mason, P.R., 2003. Single foraminiferal test chemistry records the marine environment. Geology 31, 355–358.
Sadekov, A., Eggins, S.M., Deckker, P.D., Kroon, D., 2008. Uncertainties in seawater thermometry deriving from intratest and intertest Mg/Ca variability in *Globigerinoides ruber*. Paleoceanography 23 PA1215.
Sadekov, A., Eggins, S.M., Deckker, P.D., Ninnemann, U., Kuhnt, W., Bassinot, F., 2009. Surface and subsurface seawater temperature reconstruction using Mg/Ca microanalysis of planktonic foraminifera *Globigerinoides ruber, Globigerinoides sacculifer, and Pulleniatina obliquiloculata*. Paleoceanography 24 PA3201.
Schouten, S., Hopmans, E.C., Schefuß, E., Sinninghe Damsté, J.S., 2002. Distributional variations in marine crenarchaeotal membrane lipids: a new tool for reconstructing ancient sea water temperatures? Earth Planet. Sci. Lett. 204, 265–274.
Schouten, S., Forster, A., Panoto, F.E., Sinninghe Damsté, J.S., 2007. Towards calibration of the TEX_{86} palaeothermometer for tropical sea surface temperatures in ancient greenhouse worlds. Org. Geochem. 38, 1537–1546.
Sexton, P.F., Wilson, P.A., Pearson, P.N., 2006. Palaeoecology of late middle Eocene planktic foraminifera and evolutionary implications. Mar. Micropaleontol. 60, 1–16.
Shackleton, N., Boersma, A., 1981. The climate of the Eocene ocean. J. Geol. Soc. 138, 153–157.
Speelman, E.N., Van Kempen, M.M.L., Barke, J., Brinkhuis, H., Reichart, G.J., Smolders, A.J.P., Roelofs, J.G.M., Sangiorgi, F., de Leeuw, J.W., Lotter, A.F., Sinninghe Damsté, J.S., 2009. The Eocene Arctic Azolla bloom: environmental conditions, productivity and carbon drawdown. Geobiology 7, 155–170.
Stanley, S.M., Hardie, L.A., 1998. Secular oscillations in the carbonate mineralogy of reef-building and sediment-producing organisms driven by tectonically forced shifts in seawater chemistry. Palaeogeogr. Palaeoclimatol. Palaeoecol. 144, 3–19.
Tripati, A., Elderfield, H., 2005. Deep-sea temperature and circulation changes at the Paleocene–Eocene Thermal Maximum. Science 308, 1894–1898.
Tripati, A.K., Delaney, M.L., Zachos, J.C., Anderson, L.D., Kelly, D.C., Elderfield, H., 2003. Tropical sea-surface temperature reconstruction for the early Paleogene using Mg/Ca ratios of planktonic foraminifera. Paleoceanography 18, 1101.
Tripati, A., Backman, J., Elderfield, H., Ferretti, P., 2005. Eocene bipolar glaciation associated with global carbon cycle changes. Nature 436, 341–346.
Wei, G., Laing, Z., Wen-Feng, D., Xian-Hua, L., Ying, L., Jian-Feng, C., 2009. Mn/Ca ratio in planktonic foraminifer from ODP Site 1144, the northern South China Sea: a possible paleoclimate indicator. Geochem. J. 43, 235–246.

Weldeab, S., Schneider, R.R., Kölling, M., 2006. Comparison of foraminiferal cleaning procedures for Mg/Ca paleothermometry on core material deposited under varying terrigenous-input and bottom water conditions. Geochem. Geophys. Geosyst. 7 Q04P12.

Wilkinson, B.H., Algeo, T.J., 1989. Sedimentary carbonate record of calcium magnesium cycling. Am. J. Sci. 289, 1158–1194.

Zachos, J.C., Stott, L.D., Lohmann, K.C., 1994. Evolution of early Cenozoic marine temperatures. Paleoceanography 9, 353–387.

Zachos, J., Pagani, M., Sloan, L., Thomas, E., Billups, K., 2001. Trends, rhythms, and aberrations in global climate 65 Ma to Present. Science 292, 686–693.

Zachos, J.C., Schouten, S., Bohaty, S., Quattlebaum, T., Sluijs, A., Brinkhuis, H., Gibbs, S.J., Bralower, T.J., 2006. Extreme warming of mid-latitude coastal ocean during the Paleocene–Eocene Thermal Maximum: inferences from TEX_{86} and isotope data. Geology 34, 737.

Zimmermann, H., 2000. Tertiary seawater chemistry — implications from primary fluid inclusions in marine halite. Am. J. Sci. 300, 723–767.